Proceedings of the
2007 IEEE Intelligent Vehicles Symposium
Istanbul, Turkey, June 13-15, 2007

Monte Carlo based Threat Assessment: Analysis and Improvements

Simon Danielsson
Institutionen för systemteknik
Linköpings universitet
SE-581 83, Linköping
Sweden
simda058@student.liu.se

Lars Petersson
National ICT Australia
Locked Bag 8001
Canberra
Australia
lars.petersson@nicta.com.au

Andreas Eidehall
Vehicle Dynamics & Active Safety
Volvo Car Corporation
SE-405 31, Göteborg
Sweden
aeidehal@volvocars.com

***Abstract*— This paper presents improvements and extensions of a previously presented threat assessment algorithm. The algorithm uses Monte Carlo simulation to find threats in a road scene. It is shown that by using a wider sample distribution and only apply the most likely samples from the Monte Carlo simulation for the threat assessment, improved results are obtained. By using this method more realistic paths will be chosen by the simulated vehicles and more complex traffic situations will be adequately handled.**

An improvement of the dynamic model is also suggested, which improves the realism of the Monte Carlo simulations. Using the new dynamic model less false positive and more valid threats are detected.

I. INTRODUCTION

Building safer vehicles is a prime concern of todays Automotive Manufacturers. There are currently many automotive collision avoidance systems approaching the market, such as collision mitigation system [1], [2] and collision warning systems [2], [3]. These applications have in common that they try to assess one kind of threat and take action when that specific threat is detected. Broadhurst *et al.* [4] presents a framework for reasoning about the future motions of multiple objects in a road scene. This method can be used to find threats by predicting the paths of the objects using Monte Carlo simulation. Using the framework presented, in theory any kind of threat could be detected, not as in earlier work only a specific one. Eidehall *et al.* [5] developed a threat assessment algorithm based on this framework.

Eidehall's algorithm simulates the road scene three seconds forward and calculates a threat level. This could be used to warn the driver or launch an autonomous response depending on the application. [6] states that inattention of the driver during the last three seconds before the collision is a contributing factor in 93% of the crashes. Consequently, many accidents could be avoided or reduced in severity if the driver gets a warning in this time frame.

The algorithm in [5] simulates the host vehicle as a deterministic object and all other objects, in the road scene, as stochastic ones. The future paths of other objects are determined by their current position and future control inputs, such as, steering or braking. In a real application, their current positions can be measured with a sensor, or a combination of sensors. However, their future control inputs are unknown and that is why they are modelled using a stochastic variable:

$$\mathcal{U} = [\mathbf{u}_1, \ldots, \mathbf{u}_m],$$

which consists of the control input for m number of objects in the scene. $\mathbf{u}_i$ contains the control input for a time interval $I_t = [0, T_{\max}]$ for object i, *i.e.*, $\mathbf{u}_i = (u_1(t), \ldots, u_{n_c}(t))_i$. $T_{\max}$ is the prediction horizon, *i.e.*, the time period the predictions are made and n_c is the number of control inputs for each object. This means; given a control input $\mathcal{U}$, the entire system can be simulated, using motion models for all objects, to reach a state $X(\mathcal{U})$. $X(\mathcal{U})$ will contain the position and other states for all objects for the entire time interval I_t, given the control input $\mathcal{U}$, and can be written:

$$X(\mathcal{U}) = [\mathbf{x}_1(\mathbf{u}_1), \ldots, \mathbf{x}_m(\mathbf{u}_m)].$$

A threat is reported if the host vehicle need to change its intended path, in order to avoid a collision. All objects in the scene are simulated with a Monte Carlo algorithm, using an improved resampling procedure, called iterative sampling. The iterative sampling lends many ideas from particle filter resampling [7]. The samples are weighted according to how likely paths they represent and the most likely samples are used to calculate the threat level. This paper presents an analysis of and improvements in two areas, the dynamic model and the sample distribution, of the algorithm suggested in [5]. Using these improvements, more realistic paths will be chosen by the simulated samples and better performance of the threat assessment is obtained.

II. DYNAMIC MODEL

In this section the Dynamic Model is analysed and an improved model is presented. The reason why the original Dynamic Model in [5] needs to be changed is discussed.

National ICT Australia is funded by the Australian Department of Communications, Information & Technology & the Arts and the Australian Research Council through Backing Australia's ability and the ICT Centre of Excellence Program.

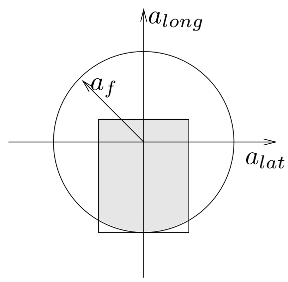

Fig. 1. The limitations of the acceleration. The acceleration for a vehicle is limited by the road friction a_f, the circle, and by the maximum steering angle and engine torque, the rectangle. The intersection of the circle and the rectangle, the shadowed area, is the allowed region of acceleration.

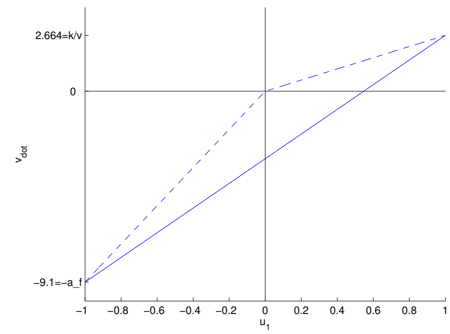

Fig. 2. The accelerations depending on the control signal u_1 for the original model (—) and the new model (- -). The plot is based on a vehicle with a velocity of 90 km/h

A. Analysis of the Original Dynamic Model

All objects in a road scene, such as cars, bicycles and pedestrians are modelled using two control inputs $(u_1,\ u_2)$ to control their longitudinal and lateral motion respectively. There are physical boundaries to the acceleration of an object, *i.e.*, for a car, engine torque and road friction. Different methods to handle these limitations have been presented in previous works. In [4], it is suggested to remove all samples with acceleration outside the boundaries from the sample set, and thereby get a physically allowed set of samples. However, in [5] it is argued that by, already from start, distributing $(u_1,\ u_2)$ according to the maximum levels of acceleration, better results can be obtained. Hence, there is no need to discard any samples, and a higher concentration of allowed control inputs is gained. Since there is a trade off between computer performance and accuracy in any Monte Carlo application it is important to not use any unnecessary computation power at this stage. With the method of Eidehall *et al.* fewer samples are required to get the same concentration of allowed samples.

The dynamic model for a car in [5] uses a simple road friction model as limitation for the acceleration, as well as maximum engine torque and maximum steering angle. The maximum road friction is described as an ellipse in the two dimensional acceleration space, and the combination of the maximum steering angle and engine torque yields a rectangle. The intersection of the ellipse and the rectangle, Figure 1, defines the allowed accelerations.

The longitudinal and lateral accelerations are treated separately and the limitations depends on the velocity of the vehicle v, and on the thresholds v_{lat} and v_{long}. The lateral acceleration is limited by the maximum steering angle φ_{max} in combination with the wheelbase L if $v \le v_{lat}$ and road friction a_f if $v > v_{lat}$. The longitudinal acceleration is limited by the engine torque k/v, where k is the engine power divided by the mass of the vehicle, if $v > v_{long}$ and road friction a_f if $v \le v_{long}$. Eidehall *et al.* argues that the breaking acceleration is limited by the road friction, not the engine torque. Therefore, the samples should be uniformly distributed between the maximum acceleration and maximum deceleration. The resulting dynamic model is:

$$\dot{x} = v\cos\theta \tag{1a}$$

$$\dot{y} = v\sin\theta \tag{1b}$$

$$\dot{v} = \begin{cases} u_1 a_f & \text{if } v \le v_{long} \\ u_1 \frac{k/v + a_f}{2} + \frac{k/v - a_f}{2} & \text{if } v > v_{long} \end{cases} \tag{1c}$$

$$\dot{\theta} = \begin{cases} v\sin\varphi_{max} u_2/L & \text{if } v \le v_{lat} \\ a_f u_2/v & \text{if } v > v_{lat} \end{cases} \tag{1d}$$

It is important that the dynamic model has correct properties such as mean values. The simulated vehicles will otherwise move in a non realistic manner. The expected mean values for the lateral and longitudinal accelerations $(\overline{acc}_{lat},\ \overline{acc}_{long})$ are zero. This is confirmed by data collected from vehicles driving on a highway. The problem with the dynamic model of Eidehall *et al.* is that Eq. (1c) has a mean lower than zero for a uniformly distributed u_1. The mean value for Eq. (1c) is:

$$\begin{aligned}\overline{acc}_{long} = \mathrm{E}[\dot{v}] &= \mathrm{E}[u_1 \frac{k/v + a_f}{2} + \frac{k/v - a_f}{2}] = \\ &= \mathrm{E}[u_1]\frac{k/v + a_f}{2} + \frac{k/v - a_f}{2} = \\ &= \{u_1 \in \mathrm{U}[-1,1],\ \mathrm{E}[u_1] = 0\} = \\ &= \frac{k/v - a_f}{2} \le 0\end{aligned} \tag{2}$$

To illustrate this a vehicle with $v_{long} = 90\ [km/h]$ is studied. As shown in Figure 2, the model has the correct min- and max-values for the acceleration but in between it is lower than expected, *i.e.*, the vehicle decelerates for $u_1 = 0$ when it is supposed to remain at the same velocity. Table I shows that the samples of the vehicle on average decelerates with about $3,2\ [m/s^2]$.

B. The improved Dynamic Model

To get a dynamic model with a more accurate mean acceleration it is suggested that Eq. (1c) is replaced with Eq. (3). This model has a much better mean acceleration than the original one, see Table I. Other improved properties are, as illustrated

Model	*Mean Acceleration*
original	$-3.2180\ m/s^2$
new	$-1.6091\ m/s^2$

TABLE I

MEAN VALUES OF ACCELERATIONS FOR A VEHICLE DRIVING WITH A VELOCITY OF 90 km/h

in Figure 2, that the samples accelerate for positive control signals and decelerate for negative ones. The mean value for the improved dynamic model is calculated in Eq. (4). The new model is evaluated in Section IV.

$$\dot{v} = \begin{cases} u_1 k/v & if\ v > v_{long}\ \&\ u_1 \geq 0 \\ u_1 a_f & else \end{cases} \tag{3}$$

$$\begin{aligned} \overline{acc}_{long} = \mathrm{E}[\dot{v}] = \{u_{1a} \in \mathrm{U}[-1,0],\ u_{1b} \in \mathrm{U}[0,1]\} = \\ = \frac{1}{2}\mathrm{E}[u_{1a}a_f] + \frac{1}{2}\mathrm{E}[u_{1b}k/v] = \\ = \frac{a_f}{2}\mathrm{E}[u_{1a}] + \frac{k/v}{2}\mathrm{E}[u_{1b}] = \\ = \{\mathrm{E}[u_{1a}] = -1/2,\ \mathrm{E}[u_{1b}] = 1/2\} = \\ = \frac{k/v - a_f}{4} \leq 0 \end{aligned} \tag{4}$$

C. Ideas of further Improvements

It is believed that a model with $\overline{acc}_{long} \approx 0$ could be found by studying the acceleration patterns of real vehicles. A model fitted like this would probably not be as simple and mathematically appealing as the one suggested.

Another way to get $\overline{acc}_{long} = 0$ is to move the breakpoint in Equation 3 from the origin to the left. Depending on the velocity it is possible to find a solution with the correct mean value. However, this method loses the feature that $u_1 = 0 \ => \dot{v} = 0$.

III. Sample Distribution

In this section the effect of the spread of the sample distribution and the percentage of samples used to calculate the threat level are studied. Two kinds of sample distributions are studied for different scenarios, firstly, the distribution generated with the Monte Carlo algorithm, called the primary distribution. Secondly, the distribution used to calculate the threat level, which is a subset of the primary distribution, that includes a percentage of the most likely samples, called the secondary distribution. A change to a more spread primary distribution with a lower percentage is suggested.

A. The Primary Distribution

Eidehall *et al.* argues that virtually all of the samples from the primary distribution should be used in the threat calculation since it is extremely unlikely for a vehicle to be involved in an accident. Compare the number of driven $[km]$ with the number of accidents. 99% of the samples' probability mass is used in the secondary distribution resulting in that only the most extreme cases are left out. To be able to work with this many samples, Eidehall *et al.* use a narrow primary sample distribution where most generated samples follows the intended path.

However, one of the reasons that vehicles veritably never crash is that the driver sees the road scene in front and anticipates its appearance in the near future. If the driver sees a static obstacle in front of the vehicle a turn or brake action will be applied to avoid it. The samples in the Monte Carlo simulation do not have this information about the surroundings and can not predict the future, they are exclusively controlled by two random input signals. To compensate for the lack of information, many more samples need to be generated to ensure that every likely path is found. These paths might be the elementary choice of a human driver whereas almost no samples in a narrow distribution will find them.

The behaviour of the primary sample distributions are effectively controlled by four behaviour parameters, λ_i, $i = [1,2,3,4]$, described by Broadhurst *et al.* The parameters control the samples' desire to follow the intended path, keep the initial velocity and accelerate in the lateral and longitudinal direction. In order to get a primary distribution narrow enough to use 99% of the samples probability mass, Eidehall *et al.* use values of the parameters much higher than the ones in [4]. The effects of the λ_i-values, on the primary distribution, are presented in Figure 3. Three plots with different behaviour parameter values, called λ_i', are studied. The results are based on the parameter values used in [5], called $\hat{\lambda}_i$. A uniform scaling, $\alpha = [\frac{1}{100}, \frac{1}{10}, 1]$, $\lambda_i' = \alpha \cdot \hat{\lambda}_i$, of all four parameters is studied, not the individual values.

It is clear that lower λ_i-values creates a much more spread primary distribution that covers a larger area of the sample space. High values yield a narrower and more dense distribution.

B. The Secondary Distribution, Simple Road Scene

Experiments were performed to study the combined effects, on the secondary distribution, of the λ_i-values and the percentage of the probability mass used. Some interesting results are presented in Figure 4. As expected, the experiments show that the secondary distribution too becomes more spread for lower λ_i-values, see Figure 4(a), 4(d) and 4(c), 4(e), as well as for higher percentages, see Figure 4(a), 4(b).

When deciding what is a good secondary distribution to use for the threat evaluation, several factors need to be considered. Firstly, it is important that the samples are following relatively close to the optimal path, or the path a human driver would choose. It is important that the distribution has some variance since a human driver do not chose exactly the same path every time. An example of a good distribution is the one that Eidehall *et al.* suggested, Figure 4(d). However, both Figure 4(b) and 4(c) have equally good behaviour.

The second criteria is that the distribution consists of enough samples to accurately evaluate the threat. This would make the distribution in Figure 4(d) much better than the ones in 4(b) and 4(c) since it uses 1330 samples instead of 84 and 192.

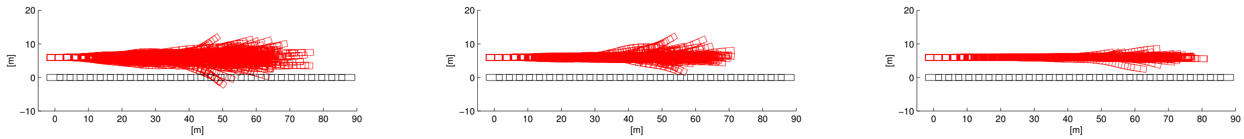

(a) $\alpha = 0.01$ (b) $\alpha = 0.1$ (c) $\alpha = 1$

Fig. 3. The effects on the primary sample distribution inflicted by the λ_i-values. The parameters are scaled uniformly with scaling $\alpha = [0.01,\ 0.1,\ 1]$. This scenario shows two vehicles travelling from left to right. The lower is the deterministic host vehicle and the upper is the stochastically modelled vehicle. The two vehicles travel in different lanes and does not constitute a threat for each other. The figure shows the entire time propagation, from 0 to 3 seconds.

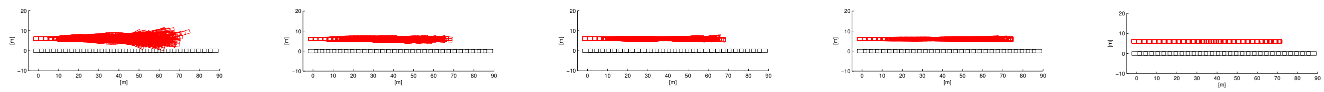

(a) $\alpha = 0.01$, 99%, number of samples: 1785 (b) $\alpha = 0.01$, 10%, number of samples: 84 (c) $\alpha = 0.1$, 30%, number of samples: 192 (d) $\alpha = 1$, 99%, number of samples: 1330 (e) $\alpha = 10$, 30%, number of samples: 129

Fig. 4. The secondary sample distribution for different scaling and percentages. These distributions are subsets of primary distribution, in Figure 3, with a percentage of the most likely samples. The scale factor, percentage and actual number of samples, out of 2000 in the primary distribution, for each secondary distribution is presented. Figure 4(d) uses the values suggested in [5].

However, the important factor is not the number of samples but rather the number of independent samples. The resampling process removes bad samples and replaces them with copies of better ones. This makes a lot of the samples in the final distribution being siblings born from a good starting sample. This effect can be observed in Figure 4(e), where the 129 samples have the same trajectory until the last resample step. This effect is present in all sample distributions but in a higher degree for higher λ_i-values.

It is hard to tell which distribution is best with just the information from the simulations of this uncomplicated scenario. In fact, it does not matter whether the secondary distribution in Figure 4(b), 4(c) or 4(d) is used in this specific case, since the differences between the distributions are so small.

C. Complicated Road Scene

To investigate the performance further, tests on a more complicated scenario were performed. This scenario is the same as the previous one except that an obstacle is placed in front of the stochastic vehicle. The results are presented in Figure 5, and the three distributions that were good in the uncomplicated scenario in section III-B are studied. Both the primary, top row, and the secondary, bottom row, distributions are presented.

The secondary distributions are studied to see if a good path is chosen. A very smooth and natural path has been found in Figure 5(a). The primary distribution is also very good, it covers the sample space well and no holes can be found. The secondary distribution in Figure 5(b) could also be a good candidate. However, it lacks some features of a human driver. If an obstacle is discovered this close in front of the vehicle, a human would immediately use a steering action to avoid it, not like in this case wait for a little bit and then do a more powerful steering. The primary Monte Carlo distribution is relatively good in this case too, but big holes can be discovered in the distribution just after the passage of the obstacle. This is because the samples mostly derive from two families with different paths.

Step	Fig. 5(a)		Fig. 5(b)		Fig. 5(c)	
	run 1	run 2	run 1	run 2	run 1	run 2
1	1000	1000	1000	1000	1000	1000
2	686	696	668	708	559	552
3	49	52	13	12	6	5
4	1000	1000	1000	254	1000	1000
5	1000	1000	1000	1000	1000	1000

TABLE II

The number of conflict free samples at the resampling steps in the Monte Carlo simulation. Three scenarios are evaluated, with results from two Monte Carlo simulations. Only the interesting resample steps around the passing of the obstacle are studied.

The secondary distribution in Figure 5(c) is not a good path, in fact it looks like two different ones. It consists mostly of siblings of two samples. The primary distribution is bad as well; it is a narrow distribution that does not cover much of the sample space.

The number of samples is studied to understand why the distributions behave the way they do. The actual number of samples used in the final distribution is not the most important factor to study, but rather the number of samples they derive from. The number of conflict free samples at the resamplings in the Monte Carlo simulation is presented in Table II. The Monte Carlo simulation has been run twice.

It is clear that the distribution in Figure 5(a) generates much more samples that finds their way around the obstacle, so its final distribution is derived from a lot more samples and should therefore have a better statistical base. The sample space gets a better coverage and more paths are examined in order to find the best one.

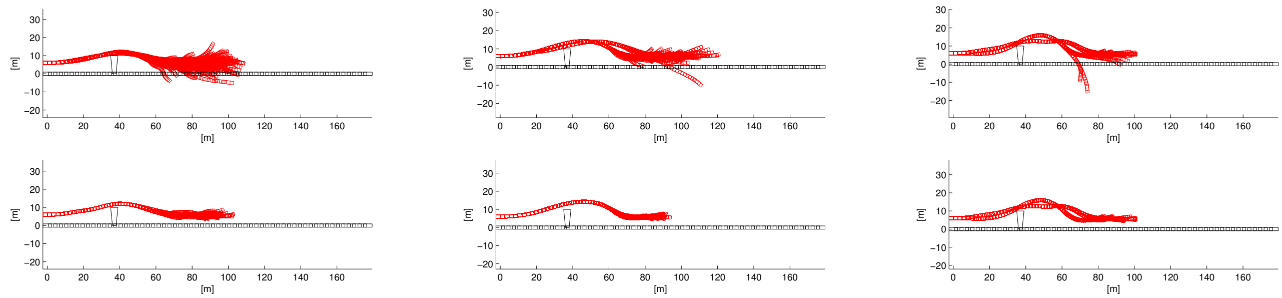

(a) $\alpha = 0.01$, 10%, number of samples: 89 (b) $\alpha = 0.1$, 30%, number of samples: 230 (c) $\alpha = 1$, 99%, number of samples: 1392

Fig. 5. The primary, top, and secondary, bottom, distributions. The scenario presented is the same on as in Figure 4 except that an obstacle has been placed in front of the stochastic vehicle. The scale factor, percentage and actual number of samples, out of 2000 in the primary distribution, for each secondary distribution is presented.

With the information from Table II it is possible to explain the appearance of Figure 5(c). Since only 5–6 survived the passage the rest of the distribution is derived from them. In this case it is even possible that two of the surviving samples has a much higher probability than the others and that almost only those ones got copied. The appearance of the primary distribution supports this theory. Having this few samples as parents for the distribution is not a good statistical basis.

It is suggested that the distribution with a scale factor, $\alpha = 0.01$ that uses 10% of the samples' probability mass is used instead of the original one suggested in [5]. The new distribution has a better appearance in a complicated scenario and it derives from more samples which improves the statistical base.

D. Overtaking Scenario

To further confirm the performance of the new distribution, an overtaking scenario is studied. A scenario where a stochastic vehicle is overtaking the host vehicle for the original and the suggested distributions are plotted in Figure 6. The new distribution has a better performance in this case too. The overtaking starts much earlier in Figure 6(a) than in 6(b), just like a human driver would do.

A close study of Figure 6(b) shows that the distribution mostly derives from just one sample that found a good way around the host vehicle. In Figure 6(a) the distribution is much denser during the overtaking and therefore more samples have found the way. This shows again that even though less samples are used in the final distribution for 6(a) than for 6(b) it has a much better statistical base.

IV. Evaluation on Traffic Data

In this section the effects of the improved dynamics and the changed sample distribution, on the threat assessment, are studied. The algorithm with the new implementations was applied on 3.5h of data collected while driving a host vehicle on a freeway.

The number of threats detected is lower using the improved dynamic model, as shown in Figure 7. The threats that have disappeared are from situations when the host vehicle is driving behind an other vehicle in the same lane with the same or higher velocity. To further study this effect, a similar test scenario, where the host vehicle is closing in on an other vehicle, was created, see Figure 8.

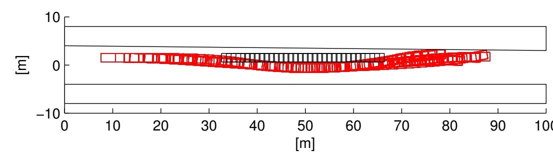

(a) $\alpha = 0.01$, 10%, number of samples: 51

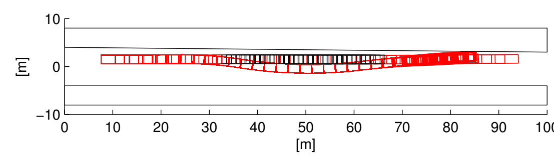

(b) $\alpha = 1$, 99%, number of samples: 764

Fig. 6. A scenario where a stochastic vehicle overtakes the deterministic host vehicle. The secondary distributions are presented.

The samples using the original dynamic model travels a shorter distance than the ones with the improved dynamic model. This makes the host vehicle drive in to some of the samples which results in a conflict. A threat is detected for the original model, with time to collision 2.7 $[s]$. No threat is detected for the scenario with the new dynamic model. This shows that the improved dynamic model has a potential of not giving as many false positive threat warnings as before. An other contribution is that more valid threats could be detected. With the improved dynamics, threats will be detected when a vehicle is closing in on the host vehicle, that the original model would overlook.

More threats were detected when using the changed sample distribution, see Figure 7. The new threats can be divided into three categories:

1) The host vehicle driving behind an other vehicle in the

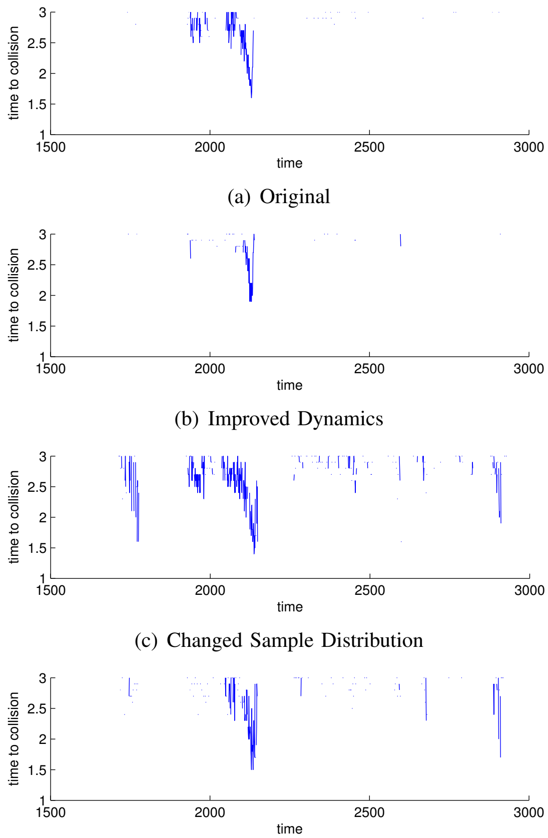

(a) Original

(b) Improved Dynamics

(c) Changed Sample Distribution

(d) Both Improved Dynamics and Changed Sample Distribution

Fig. 7. This figure shows the detected threats when the different algorithms were applied on a dataset. The data was collected while driving the host vehicle on a freeway.

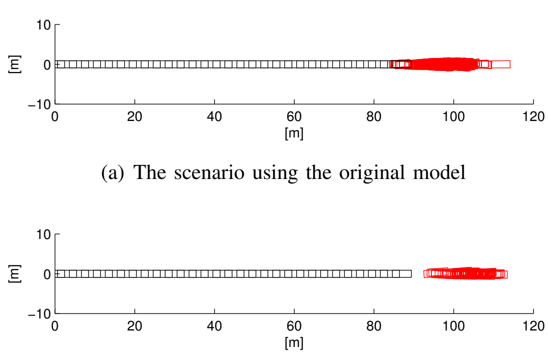

(a) The scenario using the original model

(b) The scenario using the improved dynamics model

Fig. 8. A scenario where the host vehicle is closing in on an other vehicle. The positions of the host vehicle during the whole scenario and the final position of the samples of the other vehicle is plotted. The host vehicle starts in the origin and has a velocity of 30 $[m/s]$, the other vehicle starts 35 $[m]$ in front of the host vehicle with the initial velocity of 25 $[m/s]$.

same lane.

2) The host vehicle driving close behind a vehicle near the line in an adjacent lane.
3) Two vehicles excluding the host vehicle driving close together in the same lane.

The first two kinds of new threats appear because the new distribution is a little bit more spread than the original one. These threats could in some cases be regarded as false positives. By also applying the improved dynamic model most of the new threats of the first kind disappears. The scattered threats between 2200–2800 [s] in Figure 7(c) mainly consists of the first kind and they are considerably reduced in Figure 7(d). The last threat in Figure 7(c) is of the second kind. The appearance of this sort of false threat could be solved by adjusting the individual λ_i-values and thereby get a distribution a with less lateral spread.

The third kind of threats are valid threats. The original threat assessment algorithm has a problem detecting threats that does not involve the host vehicle, since all conflict samples are removed in the iterative resampling. Being able to detect these threats demonstrates the strength of the whole framework. However the improved dynamic model reduces these threats too. The first threat in 7(c) is of the third kind and it has almost disappeared in 7(d).

V. Conclusion

Two methods to improve the threat assessment algorithm suggested by Eidehall *et al.* [5] have been presented and analysed. It has been shown that by using these methods a better performance of the threat detection is gained. Better and more realistic paths are chosen by the simulated samples and more complex traffic situation can be assessed. More valid threats can be detected and less false positives are found.

References

[1] J. Jansson, “Collision avoidance theory with applications to automotive collision mitigation,” Department of Electrical Engineering, University of Linköping, PhD Thesis 950, 2005.

[2] R. Bishop, *Intelligent Vehicle Technology and Trends*. Artech House, INC, 2005.

[3] A. Burgett, A. Carter, R. Miller, W. Najim, and D. Smith, “A collision warning algorithm for rear-end collisions,” in *16th International Technical Conference on Enhanced Safety of Vehicles*, May 1998.

[4] A. E. Broadhurst, S. Baker, and T. Kanade, “Monte carlo road safety reasoning,” in *Proceedings of the IEEE Intelligent Vehicles Symposium 2005*, Las Vegas, USA, June 2005, pp. 319–324.

[5] A. Eidehall and L. Petersson, “Threat assessment for general road scenes using monte carlo sampling,” in *Proceedings of the IEEE ITSC 2006*, September 2006, pp. 1173–1178.

[6] V. L. Neale, T. A. Dingus, S. G. Klauer, J. Sudweeks, and M. Goodman, “An overview of the 100-car naturalistic study and findings,” National Highway Traffic Safety Administration, Washingthon D.C., United States, Tech. Rep. 05-0400, 2005.

[7] J. D. Hol, “Resampling in particle filters,” Department of Electrical Engineering, University of Linköping, Tech. Rep. 283, 2004.